Multilayer Functional Tapes Co-fired at 450 °C: Beyond HTCC and LTCC Technology

Jobin Varghese*, Tuomo Siponkoski, Maciej Sobocinski, Timo Vahera and Heli Jantunen

Microelectronics Research Unit, Faculty of Information Technology and Electrical Engineering, University of Oulu, FI-90014 Oulu, Finland,

KEYWORDS (*ULTCC; Tape casting; Co-firing; Dielectric properties; Functional properties; CTE)*

ABSTRACT: This paper reports the first ultralow sintering temperature (450 °C) co-fired multifunctional ceramic substrate based on a commercial lead zirconium titanate (PZ29)-glass composite and fabricated by tape casting, isostatic lamination, and sintering. This substrate was prepared from a novel tape casting slurry composition suitable for co-firing at this low temperature with commercial Ag electrodes at 450 °C. The green cast tape and sintered substrate showed a surface roughness of 146 nm and 355 nm, respectively, suitable for device level fabrication by post-processing. Additionally, the ferroelectric and piezoelectric studies disclosed very low remnant polarization due to the dielectric glass matrix, and average values of piezoelectric coefficient (+ d_{33}), and voltage coefficient (+ g_{33}) of 17 pC/N and 30 mV/N, respectively. The dielectric permittivity and loss value of the sintered substrates were 57.8 and 0.05 at 2.3 GHz. The variation of relative permittivity on temperature dependence in the range of -40 to 80 °C was about 23 %, and the linear coefficient of thermal expansion was 6.9 ppm/°C in the measured temperature range of 100 to 300 °C. Moreover, the shelf life of the tape over 28 months was studied through measurement of the stability of the dielectric properties over time. The obtained results open up a new strategy for the fabrication of next-generation low cost functional ceramic devices prepared at ultralow temperature in comparison to the HTCC and LTCC technologies.

1. INTRODUCTION

Decreasing the sintering temperature of ceramics is attracting more and more attention for the next generation low-cost ceramic products such as multi-chip modules (MCM) [1], substrates [2], packages [3] and functional micro electro mechanical systems (MEMS) [4,5]. The ultra-low temperature co-fired ceramics (ULTCC) technology, especially, has progressed rapidly [6–11]. The ULTCC concept is nucleated from the conventional high-temperature co-fired ceramic (HTCC) and low-temperature co-fired ceramic (LTCC) technologies [12–14]. ULTCC technology has been a hot topic since 2015 [15–18], although the first material's composition was reported by Udovic *et. al.* in 2001 [19]. To date, over 200 ULTCC material compositions have been reported, divided into two categories; I (fabrication close to room temperature) and II (fabrication at 400-700 °C) based on the processing conditions[12]. So far, there have been only a few devices developed based on this concept[20] although several materials with outstanding dielectric properties suitable for microwave telecommunication applications are reported[13,21]. In addition to microwave materials, functional ceramics such as piezoelectrics are also technologically important due to their broad areas of application covering different sensing solutions, acoustic emission, sonars, flow meters, acceleration, dynamic force measurements and fuel level meters and, most recently, energy harvesting solutions [22].

Lead zirconium titanate ($PbZr_xTi_{1-x}O_3$, PZT) is the most well-known and widely used commercial piezoelectric material. There are several commercially available piezoelectric ceramics; PZ29 for example has very high coupling factors, and piezoelectric charge coefficients designed especially for high sensitivity or displacement applications [23]. Most of the PZT ceramics have sintering temperatures in the range of 1250-1350 °C [24]. However, to the best of our knowledge, no piezoelectric composition with a sintering temperature below 500 °C has been reported, except for polymer based composites and inks [25,26]. The ULTCC approach for piezoelectric material would also be extremely beneficial offering low-cost processing route with decreased thermal, mechanical and microstructural challenges, and most importantly, needing no protection against Pb volatilization. Unlike in the case of LTCC and HTCC, the low fabrication temperature of ULTCCs, especially when being below 500 °C, does not cause the volatilization of lead. This reduces the toxicity in the fabrication step. Cost effectiveness on the other hand is achieved through lower energy consumption due to the lower fabrication temperature and low cost investments for firing furnace. The present paper describes the first attempt to develop a functional PZT-glass based ULTCC composition by tape casting and co-firing at 450 °C.

However best of our knowledge we presented the very first functional ULTCC tape characterized in both radio and microwave frequency ranges along with functional properties and co-firability with commercial Ag electrodes. It is worth to notice that even in the cases of LTCC and HTCC, the most of the compositions reported have low permittivity and low dielectric loss and are meant for passive microwave components and packages [12, 13, 15]. The developed ULTCC material has wide range of applications in the field of multilayer packages with better overall stability than the polymer-ceramic composites. However, the present ULTCC still needs further research to improve the electrical performance more feasible for practical functional applications.

2. MATERIALS AND METHODS

2.1 Materials and their Process. The proposed ULTCC composite based on equal amounts in wt.% (0.56 volume fraction of PZ29 and 0.44 volume fraction of commercial glass) of commercial PZ29 (Ferro perm Piezoceramics A/S) ceramic and low melting-point sealing glass (G017, SCHOTT technical glasses with Pb_2O_3, Li_2O, Al_2O_3, and Si_2O) was prepared by conventional ball milling for 12 hrs. The particle size and surface area analyses of the powder were performed using the laser diffraction method (Beckman Coulter LS13320) and a particle surface area analyzer (G.W. Berg & Co. Micrometrics ASAP 2020).

Figure 1 shows the detailed fabrication flow chart of this process. The PZ29-glass composite powder was mixed with dimethyl carbonate (DMC; Sigma-Aldrich, St. Louis, MO) as a solvent and poly (propylene carbonate) (QPAC40; EMPOWER MATERIALS, New Castle, DE) as a binder by milling for 12 hrs. After addition of the two plasticizers, butyl benzyl phthalate (S160; Richard E. Mistler, Yardley, Pennsylvania) and polyethylene glycol (UCON 50HB2000; Richard E. Mistler), the milling was further continued for 24 hrs. The resultant slurry was cast on a silicone coated Mylar carrier tape using a 200 µm doctor blade and a laboratory caster (Unicaster 2000, Leeds, U.K.) at a speed of 0.8 m/min. The green tape was peeled from the Mylar and silver electrodes (599-E; ESL Europe, Berkshire, UK) were screen-printed and dried for 12 hrs at room temperature. Five tapes were stacked and vacuum laminated with hot isostatic pressing (75°C, 20 MPa, 10 minutes), followed by binder burnout (200-350 °C) and sintering at 450 °C.

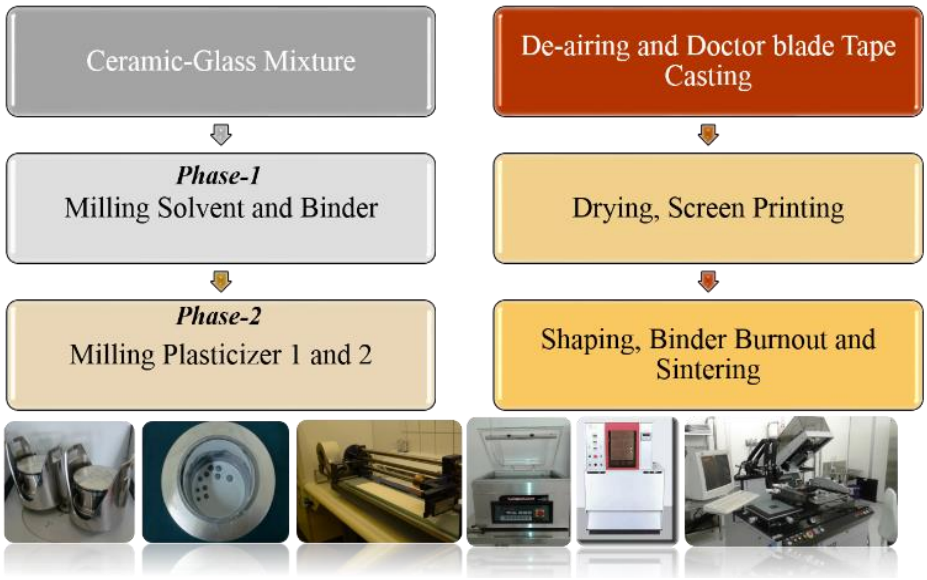

Figure 1 Tape casting processing flow chart.

2.2 Characterizations. Differential scanning calorimetric measurement (DSC)/thermogravimetric analysis (TGA) (Netzsch 404 F3, Selb, Germany) with a heating rate of 2°C/min for samples of 15.4 mg was used to study the burn out of the organic additives. Tensile strength measurements of the green tape were performed using a Temperature Controlled Tensile Strength measurement stage (TST 350, Linkam Scientific Instruments Ltd., Surrey, UK) and Linksys 32 software at room temperature with a speed of 100 µm/s using standard dumbbell-shaped samples (length 36.2 mm and width of 3.1 mm). The crystal structure and bulk density of the sintered specimens were obtained with the Archimedes method and X-ray diffractometer (Discover D8, Bruker, Germany) using Cu Kα radiation, respectively. The microstructure of the sintered sample was studied using Field Emission Scanning Electron Microscopy (FESEM, ZEISS Ultra Plus, Germany). The surface roughness of the green and sintered tapes was measured using an Atomic Force Microscope (AFM) (NTEGRA, NT-MDT, Russia). Relative permittivity (ε_r), dielectric loss ($\tan\delta$) and capacitance were measured at low frequencies using a precision LCR meter (HP 4284A, Keysight Technologies, USA).

The sintered and electrode coated PZ29-glass substrate was machined for capacitance measurements using a laser. Microwave dielectric properties of the green and sintered multilayer were measured using the split post dielectric resonator (SPDR) (QWED, Poland) technique with a Vector Network Analyzer (10 MHz - 20 GHz, Rohde & Schwarz, ZVB20, Germany). The total uncertainty in measuring the relative permittivity was about 0.5 % with a possibility to measure dielectric loss in the range of 10-5 by SPDR[27]. The temperature dependence of the microwave dielectric properties was measured using a furnace (Espec SU-261) operating at -40 to 100 °C integrated with a microwave measurement setup. Piezoelectric and ferroelectric properties were measured using the direct piezoelectric response in a Piezo d_{33} Test System (APC International, Ltd, USA) and Ferroelectric tester (Precision LC, Radiant Technologies, USA). The linear coefficient of thermal expansion (CTE) was investigated in the temperature range

of 100 to 425 °C with cylindrical samples of 8 mm × 15 mm² using a dilatometer (NETZSCH DIL 402 PC/4, Germany).

3. RESULTS AND DISCUSSION

3.1. Casting and Analysis. In tape casting, a knowledge of the particle size and specific surface area of the starting ceramic powder is crucial for good quality, strong and flexible green tapes[28,29]. In general, powders with uniform particle size distribution and a surface area of 1-15 m²/g are required for the tape casting process[28,30] enabling an optimized slurry composition. The particle size and specific surface area of the milled PZ29-glass powder were 6.6 µm and 1.0 m²/g, respectively. The optimized slurry composition for the tape casting (Table 1) contained 50 wt. % of PZ29-glass powder, 43.5 wt.% of DMC as the solvent, and 4.3 wt.% of QPAC®40 as the binder due to their low burnout temperature (peak rate of decomposition at 230-260 °C)[31]. The amount of both plasticizers, Butyl Benzyl Phthalate (BBP) and Poly Ethylene Glycol (PEG), was 1.1 wt. %.

Table 1 Optimized slurry composition for tape casting.

Materials	Compositions (wt. %)
PZ29-Glass	50
DMC-dimethyl carbonate	43.5
QPAC®40	4.3
Butyl benzyl phthalate	1.1
Polyethylene glycol	1.1

The surface quality and mechanical properties of the green tapes are the critical parameters which control the post-processing stages such as the screen printing of the top electrode and the multilayer lamination process [32–35]. Figure 2 (a) shows a photograph of the dried green tape, whose measured average thickness was in the range of 82-88 µm. The surface roughness of the green tape was 146 nm in the measured area of 10 × 10 µm (Figure 2 (b)-(c)).

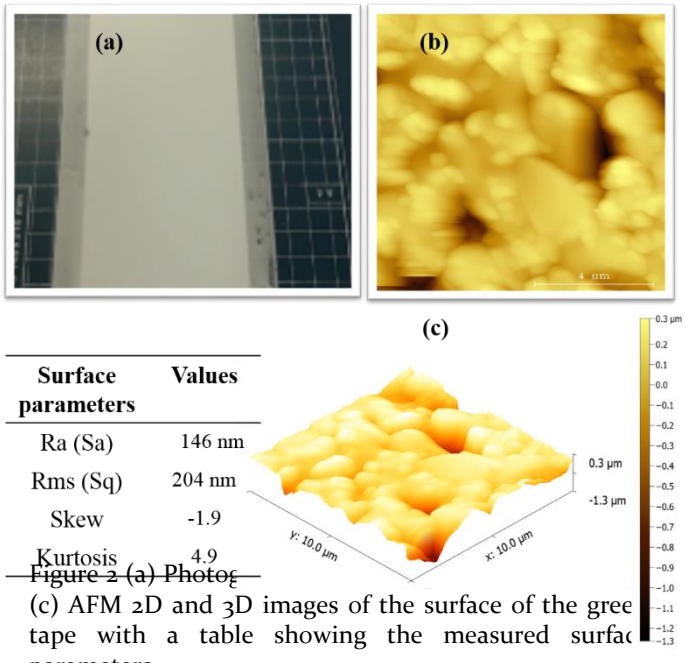

Figure 2 (a) Photog
(c) AFM 2D and 3D images of the surface of the gree
tape with a table showing the measured surfac
parameters.

The skew and kurtosis values were -1.9 and 4.9, meaning that the green tape was planar with more peaks than valleys [36]. The average tensile strength of the cast single green tape was 0.4 MPa with a standard deviation of 0.02, this being somewhat lower than that of commercial DuPont 951 tape, for example, which has a value of 1.8 MPa. The detailed green tape tensile strength comparisons of ULTCC and LTCC DuPont 951 are shown in the supporting information Table S1 (a) and (b) respectively. The poly (propylene carbonate) based binder system had a lower strength than that of other binders used in the tape casting process [28]. This is clearly due to the much lower burn out temperature. However, the developed ULTCC green tape was suitable for multilayer stacking and the screen printing process.

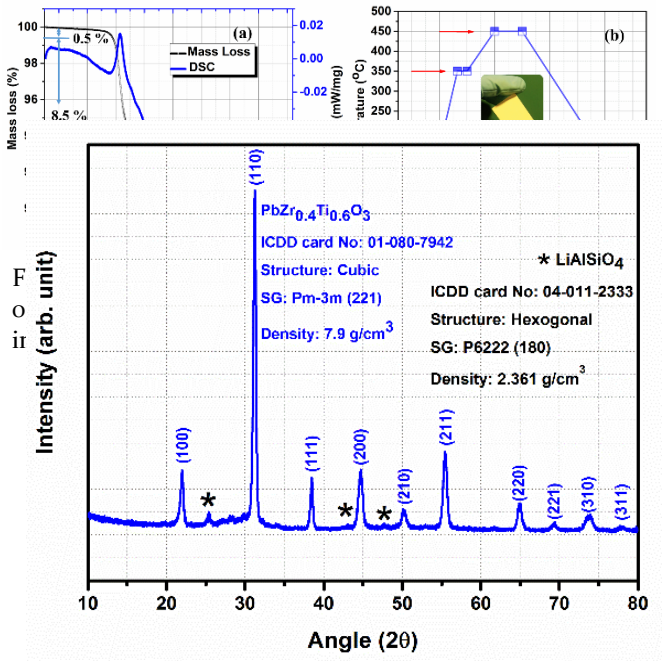

Figure 4 X-ray diffraction pattern of PZ29-glass sintered at 450 °C.

Figure 3 (a) shows the TG/DSC analysis of the green tape from room temperature to 450 °C at a heating rate of 5 °C/min. Initially, up to 150 °C, the weight loss was slow being totally 0.5 % due to moisture desorption and trapped solvent evaporation. After that it increased rapidly until 250 °C, mainly due to decomposition of carbonates from the organic additives such as the binder (QPAC®40) which was reported to happen at around 230-350 °C[31] and the plasticizers (BBP and PEG) present in the green tape [37]. The endothermic and exothermic peaks present in the DSC analysis further confirmed the decomposition of the low molecular weight binder, plasticizers and melting of low melting-point glass present in the ULTCC composition. The melting of the glass acts as the liquid phase for the PZ29 ceramics which happens at around 400-415 °C [38]. Based on these results, a sintering profile suitable for the PZ29-glass tape was designed and applied (Figure 3 (b)). The laminated 5 layer green tape had

a thickness of 400 µm. Sintering shrinkages of 12 %, 13 % and 16 % in the x, y and z-directions, respectively, were observed, with a densification of 95 % and a final thickness of 336 µm.

3.2. Structural and Microstructural Studies. Figure 4 shows the X-ray diffraction pattern of the PZ29-glass after sintering at 450 °C with the cubic lead zirconium titanate (standard ICDD card (No: 04-011-2333) of $PbZr_{0.4}Ti_{0.6}O_3$) together with a new phase of $LiAlSiO_4$ reacted from the glass composition. Previous research also reported $LiAlSiO_4$ phase formation close to the present sintering temperature of 450 °C [39].

Figure 5 shows the cross-section microstructure of the (a) sintered 5 layer laminated tape, (b) Ag co-fired at 450 °C, (c) a back scattered SEM cross-section image for EDS analysis, and the accompanying table. All the PZ29 particles (spectrum 11) were completely surrounded by a glassy phase (spectrums 10 and 12), where also small amount of Si was detected. Figure 5 (c) show also that the co-fired Ag was well attached to the ULTCC substrate. In addition, EDS line mapping analysis are provided in the supporting information Figure S1 (a), (b) and (c) for further confirming the no Ag diffusivity in the co-firing at 450 °C. The results confirm that the commercial Ag ink is well suited for the present ULTCC substrate/package material for the low temperature fabrication of electronic devices. In addition to this, the microstructure of the green tape is also present in the supporting information, Figure S2, showing the PZ29-glass particles surrounded by the organic matrix used in the casting.

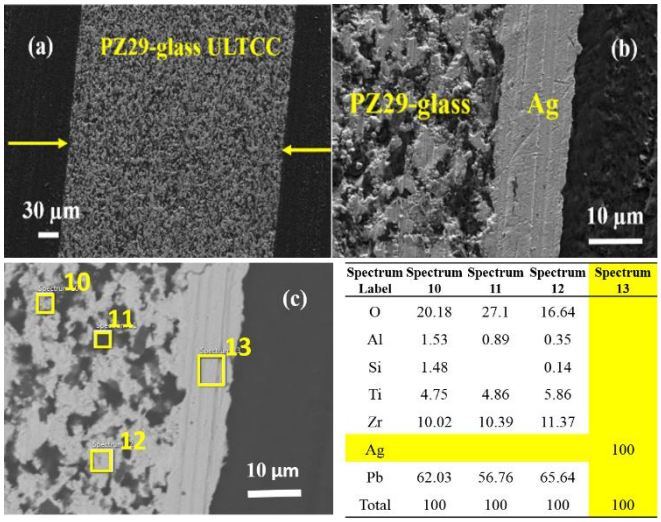

Spectrum Label	Spectrum 10	Spectrum 11	Spectrum 12	Spectrum 13
O	20.18	27.1	16.64	
Al	1.53	0.89	0.35	
Si	1.48		0.14	
Ti	4.75	4.86	5.86	
Zr	10.02	10.39	11.37	
Ag				100
Pb	62.03	56.76	65.64	
Total	100	100	100	100

Figure 5 Cross-section microstructure of ULTCC substrate sintered at 450 °C (a) five layer-laminated, (b) Ag co-fired and (c) SEM image of Ag co-fired substrate with EDS analysis results in accompanying table.

The AFM surface parameters estimated from the 2D and 3D images of a sintered PZ29-glass sample are shown in Figure S3 (a) and (b). As compared to the green tape, the average surface roughness increased to the value of ~ 355 nm, this being lower or at same level as reported for commercial LTCCs [40]. A similar trend was also observed in the RMS value while the skewness and kurtosis value were negative indicating a planar nature as well as a more uniform surface grain and valley of the grain boundaries in the glass matrix. Surface roughness analysis is desirable for substrate/package materials when post-firing of accurate conductive lines is needed or if the application is operating at high frequencies[41]. Importantly, when the surface roughness becomes of the order of the skin depth, the attenuation of transmission lines increases [42].

3.3. Low-frequency Dielectric Properties of PZ29-glass Sintered at 450 °C. Figure 6 (a) presents the variation of capacitance with varying frequency up to 1 MHz of the PZ29-glass sintered at 450 °C. It was observed that the developed ULTCC possessed a room temperature capacitance value of 121 pF measured at 1MHz. However, most ceramic capacitors are fabricated at very high sintering temperature such as the LTCC and HTCC ranges. However, ULTCC research is only in the early stages, and more research is needed in this area to enable real practical applications. An alternative option would be the embedding of these capacitors into a module made of different ULTCC compositions. This would be feasible due to the ultralow fabrication temperature.

Figure 6 inset shows the laser-processed SMD ULTCC capacitor prototypes for future electronic applications. Figure 6 (b) reveals
the dielectric properties of the ULTCC functional substrate developed before and after the poling process (electric field of 15 V/µm, poling time 5 min with the maximum temperature of 100 °C) which caused about 11 % relative permittivity variation at 1 MHz and an increase of loss tangent from 0.013 to 0.019. The low relative permittivity value of PZ29 glass is due the low permittivity (~ 12.8 at high

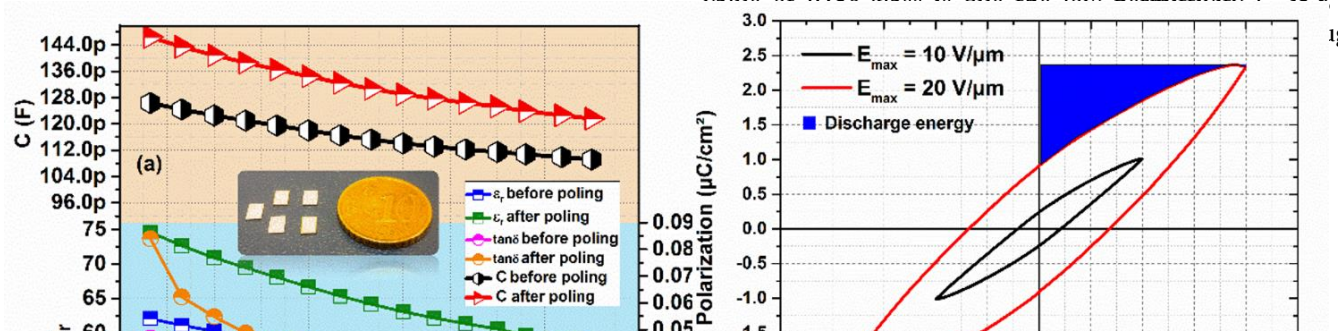

3.4. Ferroelectric, Energy Storage and Piezoelectric Studies of Developed Functional ULTCC. The P-E hysteresis loop and discharge energy of a sample under maximum fields of 10 and 20 V/μm are shown in Figure 6 (c). The average maximum polarization (P_{max}) and remnant polarization (P_r) were ~ 2.2 μC/cm2 and ~ 0.81 μC/cm², respectively. The developed sample possessed non-linear polarization and ferroelectric properties with a low value of remnant polarization (0.8 μC/cm², at 20 V/μm and 2.5 Hz) as shown in Table 2.

Table 2 Average ferroelectric properties with a standard deviation of developed ULTCC PZ29-glass.

Ferroelectric properties	P_{max} (μC/cm²)	P_r (μC/cm²)	$-P_r$ (μC/cm²)
Average	2.2	0.8	-0.8
Standard deviation	5 %	~8.75 %	~8.75 %

The studied samples did not achieve saturated behavior even at a high electric field (20 V/μm). The low polarization is due to the low coupling of the electric field between the high permittivity ceramic particles and the low permittivity matrix (0-3 connection) as well as the fact that there is only 56 vol.% ferroelectric ceramic filler in the material. The maximum electric field that the material could withstand without a breakdown in PE measurements was notably higher than that for bulk ceramics, which indicates that the filler particles were well distributed in the material[43].

The energy storage properties as described by the energy density (J) of the developed ULTCC in an electric field can be calculated by integrating the discharge curve of the PE–loop against the polarization (y-axis) [44],

$$J = \int E \, dP \qquad (1)$$

where J is the energy density, E is the electric field and P is polarization. The stored energy density (Js) is equal to the area between the y-axis and the charging polarization curve, while the discharge energy (Jd) can be calculated by integrating the area between the discharging polarization curve and the y-axis (blue area in Figure 6 (c)). The average energy densities at 10 and 20 V/μm were 0.33 J/cm³ and 0.12 J/cm³ respectively. The ratio between these gives an energy efficiency of 36.2 %. This low level of efficiency can be understood as being due to the hysteresis losses of the ferroelectric filler and the interfacial polarization.

The low permittivity matrix and high permittivity filler may create extra polarization at the matrix-filler interfaces. These interfacial polarizations have two well-known properties; they increase permittivity at low frequency but decrease the discharged energy in P–E loops due to the longer relaxation time and the trapping of charges at the interfaces [45,46] The unreleased energy can be seen in Figure 6 (c) as the area between the charge and discharge curves. Nevertheless, these results represent the highest values reported for ULTCC materials so far, and they are very comparable with some ceramic-glass capacitor materials (fabrication temperatures >800 °C) [46,47]. Higher energy densities and efficiency could be reached by changing the filler to a material developed for energy storage applications [48–50].

Table 3 The average values of piezoelectric response of the ULTCC multilayer functional substrate.

Piezo/dielectric properties	$+d_{33}$ (pC/N)	ε_r@1 kHz	tanδ @1kHz	$+g_{33}$ mV/N
Average	17.3	65	0.03	30
Standard deviation	0.6	1.4	0.004	0.5

PZ29 is a piezoelectric material; the PZ29-glass substrate also showed some piezoelectric properties (Table 3) having an average d_{33} of 17.3 pC/N at 110 Hz (the excitation frequency of the piezometer). The estimated voltage coefficient ($+g_{33}$) was 30 mV/N (at 1 kHz), which indicated that the developed material could also be suitable for sensor applications with some further research. As for comparison, the g_{33} of PZT thick film fired on LTCC (ε_r at 1 kHz 195, d_{33} 30 pC/N) and alumina (ε_r at 1 kHz 521, d_{33} 120 pC/N) substrates is 17 and 26 mV/N, respectively [51]. The g_{33} of the bulk PZ29 is reported to be 23 mV/N, which is lower than that calculated with the developed glass substrate. However it must be kept in mind that the d_{33} of PZ29 is as high as 575 due to its high permittivity of PZ29 bulk sample (2900 at 1 kHz) [52].

3.5. Microwave Dielectric Properties of Green Tape and Sintered Substrates. To study the shelf life of the green tape, its dielectric properties were measure as a function of storage time, which indicated the stability of the developed slurry composition. After casting, the green tape showed a relative permittivity of 12.9 and 12.6 and dielectric loss of 0.07 and 0.08, respectively at 2.4 and 5.1 GHz (Table S2). The difference compared to the sintered multilayer substrate, having a permittivity and dielectric loss of 57.8 and 0.05 at 2.4 GHz, is due to the organic additives present in the green tape. However, the sintered multilayer substrate did not

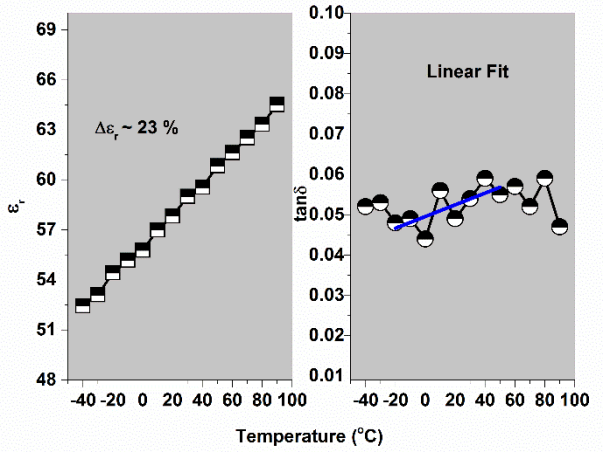

Figure 7 Sintered ULTCC substrate temperature dependence of relative permittivity and dielectric loss at 2.4 GHz.

show resonance at 5.1 GHz and so the values were not accessible.

The shelf life of the green single layer tape in terms of its microwave dielectric properties at 2.4 and 5.1 GHz is shown in Figure S4. The ageing measured over 28 months (Figure S4) showed only about a 0.3-0.4 % variation in the relative permittivity and 10 % variation in the dielectric loss measured at 2.4 and 5.1 GHz respectively. The relative permittivity and dielectric loss error bars are assigned based on the SPDR accuracy as well as the calibration at different intervals of time. These results are important to describe the predicted shelf life of ULTCC tape for long-term storage and usages. However, the mechanical properties of the tapes as a function of storage time need further research.

Figure 7 shows the temperature dependence of relative permittivity and dielectric loss at 2.4 GHz. The relative permittivity increased with increase in the temperature range while the dielectric loss showed an abnormal variation, which was expected and may be due to the high interaction of thermal vibrations on its electronic /ionic polarization in the microwave frequency range. The sintered ULTCC substrate showed a variation of relative permittivity of about 23 % in the temperature range of -40 to 90 °C. The dielectric loss value was linear fitted to estimate the approximate temperature variation in dielectric loss at microwave frequency. The dielectric loss also increased with increase in temperature as expected.

The present studies reveal that the ULTCC technology opens up a new path for low-cost fabrication of multilayer packages/substrates fabrication at 450 °C, which is much closer to room temperature than of HTCC or LTCC technology.

3.6. Linear Coefficient of Thermal Expansion of the Sintered PZ29-glass at 450 °C. Figure 8 (a) and (b) shows the variation of linear change in dimensions within the temperature range ((a) heating and (b) cooling cycle) of 100-300 °C. The calculated linear CTE of 7.4 ppm/°C was observed in the heating cycle (100 to 300 °C) of the measured temperature ranges. The cooling cycle, (300-100 °C) showed a similar trend with an average linear CTE of 6.5 ppm/°C. The variations of linear CTE of the ULTCC sample at selected temperature ranges in the heating and cooling cycle were also calculated and are shown in the inset tables of figure 8.

The CTE plays an important role in the device level integration, especially during co-firing of two materials. In multilayer structures controlling thermal delamination is one of the major challenge. In order to control the thermal delamination when co-firing, the CTE matching with metals is needed [53, 54]. Careful selection of commercial grade Ag paste having the same firing temperature the developed ULTCC was done. Both of the materials being in a soft stage during the firing minimizes problems caused by the CTE difference. The feasibility of the selected Ag paste in this sense was also evident from the microstructure (figure 5 (c).

4. CONCLUSION

The present paper reports a new strategy for multi-functional materials through ULTCC technology. A low-cost fabrication method for new functional ULTCC multilayer structures co-fired with Ag at 450 °C and possessing moderate dielectric, piezoelectric and ferroelectric properties for future low-cost multilayer packages was demonstrated for the first time. The developed PZ29-glass was cast in green tape using a binder system and co-fired below 500 °C. A systematic sintering profile was optimized based on TG-DSC analysis and produced a uniform microstructure and 95 % densification. The sintered ULTCC substrate had a low surface roughness (355 nm). The measured voltage coefficient (+g_{33}) was 30 mV/N (at 1 kHz), which indicates that the developed material could be feasible

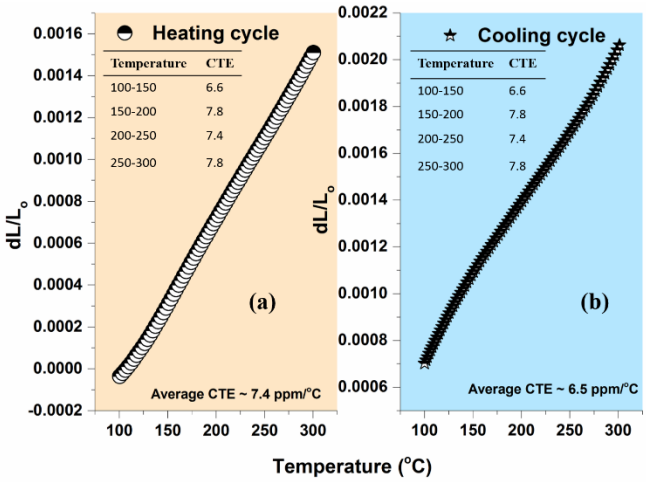

Figure 8 Variation of linear change in dimension with respect to temperature (100-300 °C) of PZ29-glass sintered at 450 °C (a) heating cycle and (b) cooling

for some sensor applications with further research. At microwave frequencies (2.4 GHz) the substrate showed a relative permittivity of 57.8 and a dielectric loss of 0.05. Moreover, the sintered PZ29-glass material exhibited an average linear CTE of 6.9 ppm/°C in the measured temperature range of 100-300 °C. The stability of the green

tape as a function of storage time through dielectric properties was also briefly studied, being an important parameter for commercial fabrication. The results reveal an important step on the way to future multilayer ULTCC production.

ASSOCIATED CONTENT

Supporting Information. Table S1 (a) Tensile strength of cast green tape with polycarbonate based binder system, (b) tensile strength of commercial DuPont 951 tape, and Table S2 The microwave dielectric properties of green single tape and 4 layer isostatic laminated tapes. Figure S1 EDS line-mapping analysis of ULTCC with Ag electrode co-fired at 450 ^{o}C. Figure S2 SEM microstructure of green tape surface (a) and (b) magnified image, Figure S3 AFM image of (a) 2D and (b) 3D with inset table of surface parameters, of a sintered PZ29-glass and Figure S4 Ageing effect of microwave dielectric properties of ULTCC single layer green tape at 2.4 and 5.1 GHz.

AUTHOR INFORMATION

Corresponding Author

*Jobin Varghese
Email: jobin.var@gmail.com
Phone: +358-0449141866

Author Contributions

The manuscript was written through contributions of all authors.

ACKNOWLEDGMENT

Authors are grateful to European Research Council Project No: 24001893 for financial support. Dr. Jobin Varghese thankful to Ulla Tuominen Foundation project grant 2018.

ABBREVIATIONS

ULTCC, ultra-low temperature co-fired ceramics, LTCC, low-temperature co-fired ceramics; HTCC, high temperature co-fired ceramics; SPDR, split-post dielectric resonator; AFM, atomic force microscopy; CTE, coefficient of thermal expansion; ppm, parts per million; SEM, scanning electron microscopy; SMD, surface mound device; TG, thermos gravimetric; DSC, differential scanning calorimetric; BBP, butyl benzyl phthalate ; PEG, polyethylene glycol.

REFERENCES

(1) R. R. Tummala, E. J. Rymaszewski; A. G. Klopfenstein. *Microelectronics Packaging Handbook*; Springer US, 1997.

(2) Imanaka, Y. *Multilayered Low Temperature Cofired Ceramics Technology*; Springer, Japan, 2005.

(3) R. R. Tummala. Ceramic and Glass-Ceramic Packaging in the 1990s. *J. Am. Ceram. Soc.* **1991**, *74*, 895–908.

(4) Sobociński, M.; Zwierz, R.; Juuti, J.; Jantunen, H.; Golonka, L. Electrical and Electromechanical Characteristics of LTCC Embedded Piezoelectric Bulk Actuators. *Adv. Appl. Ceram.* **2010**, *109* (3), 135–138.

(5) Gebhardt, S.; Partsch, U.; Schönecker, A. PZT Thick Films for MEMS. In *IEEE International Symposium on Applications of Ferroelectrics*; 2008; Vol. 2.

(6) Joseph, N ; Varghese, J.; Siponkoski, T ; Teirikangas, M ; Sebastian, M. T.; Jantunen H. Glass Free $CuMoO_4$ Ceramic with Excellent Dielectric and Thermal Properties for Ultra-Low Temperature Cofired Ceramic Applications. *ACS Sustain. Chem. Eng.* **2016**, *4* (10), 5632–5639.

(7) Varghese, J.; Siponkoski, T.; Teirikangas, M.; Sebastian, M. T.; Uusimäki, A.; Jantunen, H. Structural, Dielectric, and Thermal Properties of Pb Free Molybdate Based Ultralow Temperature Glass. *ACS Sustain. Chem. Eng.* **2016**, *4* (7), 3897-3904.

(8) Varghese, J.; Siponkoski, T.; Nelo, M.; Sebastian, M. T.; Jantunen, H. Microwave Dielectric Properties of Low-Temperature Sinterable α-MoO_3. *J. Eur. Ceram. Soc.*2017, *38* (4), 1541-1547.

(9) Chen, M. Y.; Juuti, J.; Hsi, C. S.; Chia, C. T.; Jantunen, H. Dielectric $BaTiO_3$-BBSZ Glass Ceramic Composition with Ultra-Low Sintering Temperature. *J. Eur. Ceram. Soc.* **2015**, *35* (1), 139–144.

(10) Chen, M.-Y.; Juuti, J.; Hsi, C.-S.; Chia, C.-T.; Jantunen, H. Dielectric Properties of Ultra-Low Sintering Temperature Al_2O_3-BBSZ Glass Composite. *J. Am. Ceram. Soc.* **2015**, *98* (4), 1133–1136.

(11) Chen, M. Y.; Vahera, T.; Hsi, C. S.; Sobocinski, M.; Teirikangas, M.; Peräntie, J.; Juuti, J.; Jantunen, H. Tape Casting System for ULTCCs to Fabricate Multilayer and Multimaterial 3D Electronic Packages with Embedded Electrodes. *J. Am. Ceram. Soc.* **2017**, *100* (4), 1257–1260.

(12) Sebastian, MT, Wang, H, Jantunen, H. Low Temperature Co-Fired Ceramics with Ultra-Low Sintering Temperature: A Review. *Curr. Opin. Solid State Mater. Sci.* **2016**, *20*, 151–170.

(13) Sebastian, MT, Jantunen, H. High Temperature Cofired Ceramic (HTCC), Low Temperature Cofired Ceramic (LTCC), and Ultralow Temperature Cofired Ceramic (ULTCC) Materials, In *Chapter-8, Microwave Materials and Applications Volume-1*; John Wiley & Sons Ltd., 2017.

(14) Zhao, S.; Jiang, B.; Maeder, T.; Muralt, P.; Kim, N.; Matam, S. K.; Jeong, E.; Han, Y. L.; Koebel, M. M. Dimensional and Structural Control of Silica Aerogel Membranes for Miniaturized Motionless Gas Pumps. *ACS Appl. Mater. Interfaces* **2015**, *7* (33), 18803–18814.

(15) Sebastian, M. T.; Wang, H.; Jantunen, H. Low Temperature Co-Fired Ceramics with Ultra-Low Sintering Temperature: A Review. *Current Opinion in Solid State and Materials Science*. 2016, pp 151–170.

(16) Valant, M.; Popović, J.; Mihelj, M. V.; Burazer, S.; Altomare, A.; Moliterni, A. Oxide Crystal Structure with Square-Pyramidally Coordinated Vanadium for Integrated Electronics Manufactured at Ultralow Processing Temperatures. *ACS Sustain. Chem. Eng.* **2017**, *5* (7), 5662–5668.

(17) Zhou, D.; Li, W.-B.; Guo, J.; Pang, L.-X.; Qi, Z.-M.; Shao, T.; Xie, H.-D.; Yue, Z.-X.; Yao, X. Structure, Phase Evolution, and Microwave Dielectric Properties of $(Ag_{0.5}Bi_{0.5})(Mo_{0.5}W_{0.5})O_4$ Ceramic with Ultralow Sintering Temperature. *Inorg. Chem.* **2014**, *53* (11), 5712–5716.

(18) Zhu, X.; Wang, Z.; Su, X.; Vilarinho, P. M. New Cu_3TeO_6 Ceramics: Phase Formation and Dielectric Properties. *ACS Appl. Mater. Interfaces* **2014**, *6* (14), 11326–11332.

(19) Udovic, M.; Valant, M.; Suvorov, D. Dielectric Characterisation of Ceramics from the TiO_2-TeO_2 System. *J. Eur. Ceram. Soc.* **2001**, *21* (10), 1735–1738.

(20) Kähäri, H.; Ramachandran, P.; Juuti, J.; Jantunen, H. Room-Temperature Densified Li_2MoO_4 Ceramic Patch Antenna and the Effect of Humidity. *Int. J. Appl. Ceram. Technol.* **2016**, *6*, 1–6.

(21) Joseph, N.; Varghese, J.; Teirikangas, M.; Sebastian, M. T.; Jantunen, H. $CuMoO_4$ Ceramics with Ultra-Low Sintering Temperature through Ag_2O Addition for Millimetre Wave Applications. *Compos. Part B* **2018**, *141* (December 2017), 1–18.

(22) Uchino, K. *Ferroelectric Devices & Piezoelectric Actuators*; DEStech Publication Inc., 2017.

(23) Heinonen, E.; Juuti, J.; Jantunen, H. Characteristics of Piezoelectric Cantilevers Embedded in LTCC. *J. Eur. Ceram. Soc.* **2007**, *27* (13–15), 4135–4138.

(24) Corker, D. L.; Whatmore, R. W.; Ringgaard, E.; Wolny, W. W. Liquid-Phase Sintering of PZT Ceramics. *J. Eur. Ceram. Soc.* **2000**, *20* (12), 2039–2045.

(25) Gowdhaman, P.; Antonyraj, K.; Annamalai, V. An Effective Approach on Physical and Dielectric Properties of PZT- PVDF Composites. *Int. J. Adv. Sci. Res. Int. J. Adv. Sci. Res. J.* **2015**, *1* (8), 322–328.

(26) Siponkoski, T.; Nelo, M.; Palosaari, J.; Peräntie, J.; Sobocinski, M.; Juuti, J.; Jantunen, H. Electromechanical Properties of PZT/P(VDF-TrFE) Composite Ink Printed on a Flexible Organic Substrate. *Compos. Part B Eng.* **2015**, *80*, 217–222.

(27) Krupka, J.; Gregory, a. P.; Rochard, O. C.; Clarke, R. N.; Riddle, B.; Baker-Jarvis, J. Uncertainty of Complex Permittivity Measurements by Split-Post Dielectric Resonator Technique. *J. Eur. Ceram. Soc.* **2001**, *21* (15), 2673–2676.

(28) Mistler, R. E. and Twiname, E. R. *Tape Casting: Theory and Practice*; The American Ceramic Society, 735 Ceramic Place, Westerville, Ohio 43081, 2000.

(29) Liu, Z.; Wang, Y.; Li, Y. Combinatorial Study of Ceramic Tape-Casting Slurries. *ACS Comb. Sci.* **2012**, *14* (3), 205–210.

(30) Jantunen, H.; Hu, T.; Uusimäki, A.; Leppävuori, S. Tape Casting of Ferroelectric, Dielectric, Piezoelectric and Ferromagnetic Materials. *J. Eur. Ceram. Soc.* **2004**, *24* (6), 1077–1081.

(31) Gerrit. A. Luinstra and Endres Borchardt. Material Properties of Poly(Propylene Carbonates). *Adv Polym Sci* **2012**, *254*, 29–48.

(32) Abhilash, P.; Sebastian, M. T.; Surendran, K. P. Glass Free, Non-Aqueous LTCC Tapes of Bi 4 $(SiO_4)_3$ with High Solid Loading. *J. Eur. Ceram. Soc.* **2015**, *35* (8), 2313–2320.

(33) Roshni, S. B.; Sebastian, M. T.; Surendran, K. P. Can Zinc Aluminate-Titania Composite Be an Alternative for Alumina as Microelectronic Substrate? *Sci. Rep.* **2017**, *7* (April 2016), 40839.

(34) Rajesh, S.; Jantunen, H.; Letz, M.; Pichler-Willhelm, S. Low Temperature Sintering and Dielectric Properties of Alumina-Filled Glass Composites for LTCC Applications. *Int. J. Appl. Ceram. Technol.* **2012**, *9* (1), 52–59.

(35) Arun, S.; Sebastian, M. T.; Surendran, K. P. $Li_2ZnTi_3O_8$ Based High κ LTCC Tapes for Improved Thermal Management in Hybrid Circuit Applications. *Ceram. Int.* **2017**, *43* (7), 5509–5516.

(36) Raposo, M.; Ferreira, Q.; Ribeiro, P. a. A Guide for Atomic Force Microscopy Analysis of Soft-Condensed Matter. *Mod. Res. Educ. Top. Microsc.* **2007**, 758–769.

(37) Induja, I. J.; Abhilash, P.; Arun, S.; Surendran, K. P.; Sebastian, M. T. LTCC Tapes Based on Al_2O_3-BBSZ Glass with Improved Thermal Conductivity. *Ceram. Int.* 2015, *41*(10), 13572-13581.

(38) SCOTT AG. *SCHOTT Technical Glasses Physical and Technical Properties*; 2007. (accessed on 17.01.2018)

(39) Koseva, I. I.; Tzvetkov, P. T.; Yordanova, A. S.; Marychev, M. O.; Dimitrov, O. S.; Nikolov, V. S. Preparation of Chromium Doped $LiAlSiO_4$ Glass-Ceramics. **2017**, *49* (2), 366–370.

(40) Dupont. DuPont™ GreenTape™: Design and

Layout Guidelines. **2009**, 12. (accessed on 17.01.2018)

(41) Rajesh K. B.; Subba R. T. AFM Studies on Surface Morphology, Topography and Texture of Nanostructured Zinc Aluminum Oxide Thin Films. *Dig. J. Nanomater. Biostructures* **2012**, *7* (4), 1881–1889.

(42) Bekkadal, E. O. H. and F. *A Microstrip Handbook*; University of Trondheim, Norway, 1975.

(43) Wang, X.; Zhang, Y.; Song, X.; Yuan, Z.; Ma, T.; Zhang, Q.; Deng, C.; Liang, T. Glass Additive in Barium Titanate Ceramics and Its Influence on Electrical Breakdown Strength in Relation with Energy Storage Properties. *J. Eur. Ceram. Soc.* **2012**, *32* (3), 559–567.

(44) Herczog, A. Application Of Glass-Ceramics For Electronic Components And Circuits. *IEEE Trans. Parts, Hybrids, Packag.* **1973**, *9* (4), 247–256.

(45) Hao, X. A Review on the Dielectric Materials for High Energy-Storage Application. *J. Adv. Dielectr.* **2013**, *3* (1), 1330001.

(46) Zhang, Y.; Huang, J.; Ma, T.; Wang, X.; Deng, C.; Dai, X. Sintering Temperature Dependence of Energy-Storage Properties in (Ba,Sr)TiO_3 Glass-Ceramics. *J. Am. Ceram. Soc.* **2011**, *94* (6), 1805–1810.

(47) Patel, S.; Chauhan, A.; Kundu, S.; Madhar, N. A.; Ilahi, B.; Vaish, R.; Varma, K. B. R. Tuning of Dielectric, Pyroelectric and Ferroelectric Properties of $0.715Bi_{0.5}Na_{0.5}$ TiO_3-$0.065BaTiO_3$-$0.22SrTiO_3$ Ceramic by Internal Clamping. *AIP Adv.* **2015**, *5* (8), 0–17.

(48) Wang, H.; Liu, J.; Zhai, J.; Shen, B.; Pan, Z.; Liu, J. R.; Yang, K. Effect of Crystallization Temperature on Dielectric and Energy-Storage Properties in SrO-Na_2O-Nb_2O_5-SiO_2 Glass-Ceramics. *Ceram. Int.* **2017**, *43* (12), 8898–8904.

(49) Zhang, W.; Wang, J.; Xue, S.; Liu, S.; Shen, B.; Zhai, J. Effect of La_2O_3 Additive on the Dielectric Properties of Barium Strontium Titanate Glass-Ceramics. *J. Mater. Sci. Mater. Electron.* **2014**, *25* (9), 4145–4149.

(50) Chen, K.; Pu, Y.; Xu, N.; Luo, X. Effects of SrO-B_2O_3-SiO_2 Glass Additive on Densification and Energy Storage Properties of $Ba_{0.4}Sr_{0.6}TiO_3$ Ceramics. *J. Mater. Sci. Mater. Electron.* **2012**, *23* (8), 1599–1603.

(51) Hrovat, M.; Belavič, D.; Uršič, H.; Kita, J.; Holc, J.; Drnovšek, S.; Cilenšek, J.; Kosec, M.; Moos, R. An Investigation of Thick-Film Materials for Temperature and Pressure Sensors on Self-Constrained LTCC Substrates. *Proc. - 2008 2nd Electron. Syst. Technol. Conf. ESTC* **2008**, 339–345.

(52) Ferroperm. High Quality Components and Materials for the Electronic Industry. (accessed on 17.01.2018).

(53) Arun, S.; Sebastian, M.T.;Surendran, K.P.; $Li_2ZnTi_3O_8$ based high K LTCC tapes for improved thermal management in hybrid circuit applications. Ceram. Int. 2017, *43*, 5509-5516.

(54) Joseph, N.; Varghese, J.; Teirikangnas, M.; Sebastian, M.T.; Jantunen, H.; Ultra-low sintering temperature ceramic composites of $CuMoO_4$ through Ag_2O addition for microwave applications. Composites: Part B 2018, *141*, 214-220.

Insert Table of Contents artwork

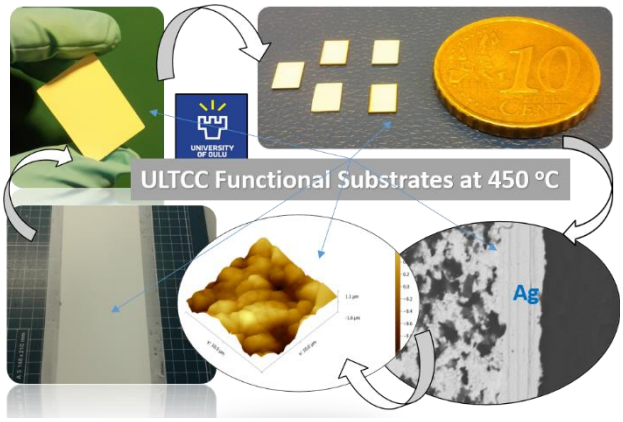
ULTCC Functional Substrates at 450 °C
Ag